RECENT RESULTS FROM THE PEP4-TPC ON QUARK FRAGMENTATION

Werner Hofmann

Representing the PEP-4 TPC Collaboration [1]

Lawrence Berkeley Laboratory
University of California
Berkeley, California 94720

November 12, 1983

---

[1] Members of the TPC Collaboration are:

H. Aihara(6), M. Alston-Garnjost(1), D.H. Badke(4), J.A. Bakken(4), A. Barbaro-Galtieri(1), A.V. Barnes(1), B.A. Barnett(4), B. Blumenfeld(4), A.D. Bross(1), C.D. Buchanan(2), W.C. Carithers(1), O. Chamberlain(1), C. Chen(1), J. Chiba(6), C-Y. Chien(4), A.R. Clark(1), O.I. Dahl(1), C.T. Day(1), P. Delpierre(1), K.A. Derby(1), P.H. Eberhard(1), D.L. Fancher(1), H. Fujii(6), T. Fujii(6), B. Gabioud(1), J.W. Gary(1), W. Gorn(3), W. Gu(1), N.J. Hadley(1), J.M. Hauptman(2), B. Heck(1), H.J. Hilke(1), W. Hofmann(1), J.E. Huth(1), J. Hylen(4), H. Iwasaki(1), T. Kamae(6), R.W. Kenney(1), L.T. Kerth(1), R.I. Koda(2), R.R. Kofler(5), K.K. Kwong(3), J.G. Layter(3), C.S. Lindsey(3), S.C. Loken(1), G.W. London(1), X-Q. Lu(4), G.R. Lynch(1), L. Madansky(4), R.J. Madaras(1), R. Majka(7), J. Mallet(1), P.S. Martin(1), K. Maruyama(6), J.N. Marx(1), J.A.J. Matthews(4), S.O. Melnikoff(3), W. Moses(1), P. Nemethy(1), D.R. Nygren(1), P.J. Oddone(1), D.A. Park(2), A. Pevsner(4), M. Pripstein(1), P.R. Robrish(1), M.T. Ronan(1), R.R. Ross(1), F.R. Rouse(1), R.R. Sauerwein(1), G. Shapiro(1), M.D. Shapiro(1), B.C. Shen(3), W.E. Slater(2), M.L. Stevenson(1), D.H. Stork(2), H.K. Ticho(2), N. Toge(6), M. Urban(1), R.F. van Daalen Wetters(2), G.J. VanDalen(3), R. van Tyen(1), H. Videau(1), M.R. Wayne(2), W.A. Wenzel(1), M. Yamauchi(6), M.E. Zeller(7), W-M. Zhang(4)

(1) Lawrence Berkeley Laboratory, Berkeley, CA 94720
(2) University of California, Los Angeles, CA 90024
(3) University of California, Riverside, CA 92521
(4) Johns Hopkins University, Baltimore, MD 21218
(5) University of Massachusetts, Amherst, MA 01003
(6) University of Tokyo, Tokyo, JAPAN
(7) Yale University, New Haven, CT 06520

Presented at the
SLAC Summer Institute on Particle Physics
Stanford, CA
August 16-27, 1983

1) Introduction

The PEP4-TPC detector [2] is the most recent addition to the detector arsenal at the PEP electron-positron storage ring. First completely assembled in October 1981, the TPC went into the PEP beam line early in 1982 and started regular data taking in May 1982; most of the results presented here are based on high-luminosity runs in the 1982-1983 cycle.

Among the detectors at PEP and PETRA the TPC detector has the following unique features:

1. The truly 3-dimensional tracking of charged particles in the TPC; for each point on a track, the x,y,z-coordinates are measured simultaneously. In the reconstruction of complex hadronic events this offers a major advantage over conventional detectors where tracks in space are reconstructed from 2-dimensional projections.

2. Particle identification based on ionization energy loss over almost the entire momentum range and solid angle.

3. Together with the PEP-9 forward detector system, the facility offers a nearly complete coverage down to polar angles of 30 mrad for charged and neutral particle detection.

Accordingly, the physics goals for the PEP-4/PEP-9 experiment concentrate on two areas: the fragmentation properties of quarks and gluons produced in e+e- annihilation, and the investigation of hadron production in 2-photon collisions. In this paper, only the first of these topics will be addressed.

Despite the many successes of QCD in the description of deep inelastic reactions, the basic fragmentation process of quarks and gluons is not very well understood. This lack of knowledge has been shown to jeopardize precise test of QCD, such as the accurate determination of the strong coupling constant [3]. With its ability to disentangle complex hadronic events and to identify most of the final state particles, the TPC allows new and more sensitive tests of fragmentation models.

This paper is organized as follows: following the introduction is a brief description of the detector and the particle identification by ionization energy loss. Next, the inclusive production of stable hadrons and of resonances is discussed, and limits on the inclusive production of fractional charged particles are given. The next chapter deals with a new analysis of long-range correlations in e+e- annihilation. A brief summary and outlook concludes the paper.

The data presented in this paper are prelimary, and under preparation for final publication.

2) The PEP-4 Detector

The PEP-4 detector (fig. 1) is a solenoid detector. Its subsystems, which have been described previously [4], include the TPC, inner and outer drift chambers, hexagonal and poletip electromagnetic calorimeters and muon detection chambers. In the analyses presented here, only the information from the TPC and the hexagonal calorimeters was used. For each charged track, up to 15 space points are measured in the TPC with a typical accuracy of 190 microns in x,y (the bending plane) and 350 microns in z (the beam direction). The momentum resolution at low momentum, dp/p = 6%, is limited by multiple scattering; for high momentum tracks, the resolution is typically 3.5%*p, for the present data. The hexagonal calorimeter detects photons over 45 % of the solid angle, with a typical energy resolution of 15 % at 1 GeV.

3) Particle Identification by dE/dx

Because the amount of ionization depends only on velocity and charge, particles can be identified by simultaneously measuring momentum and ionization energy loss (fig. 2a).

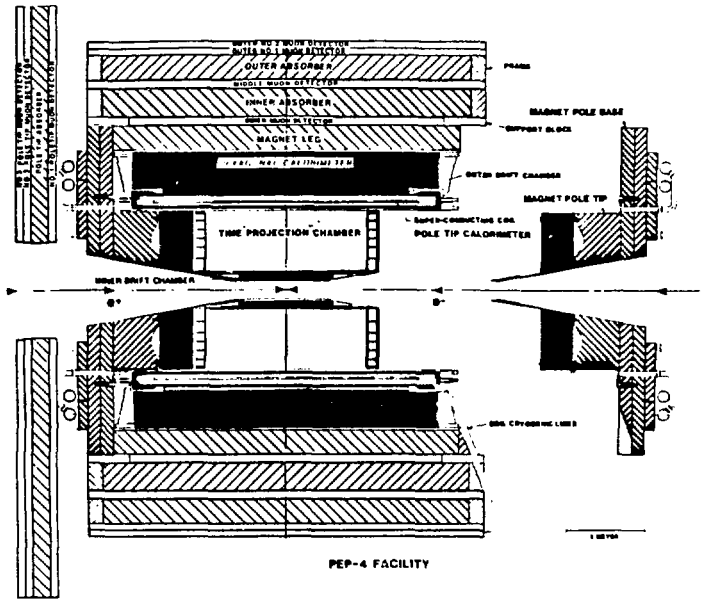

1. Cross section of the PEP-4 TPC detector, showing the different detector subsystems.

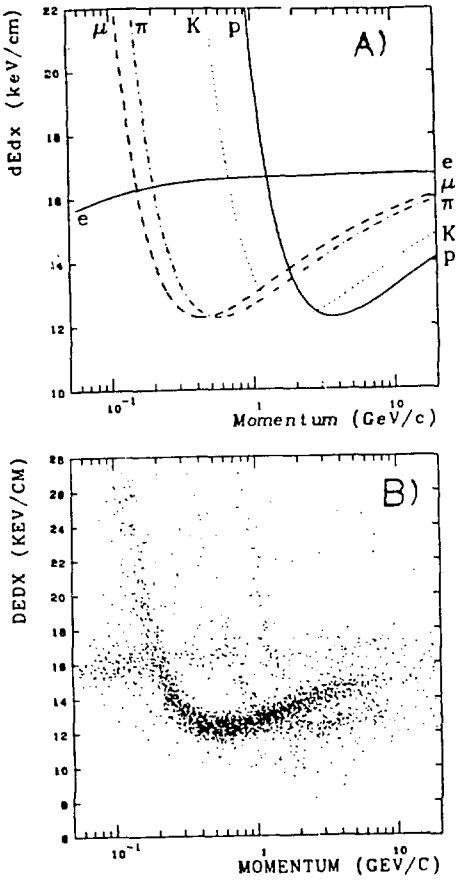

2. a) Average ionization energy loss as a function of momentum, for different particle types. b) Distribution of ionization energy loss vs. momentum for tracks in hadronic events. Only tracks with at least 80 dE/dx samples are included.

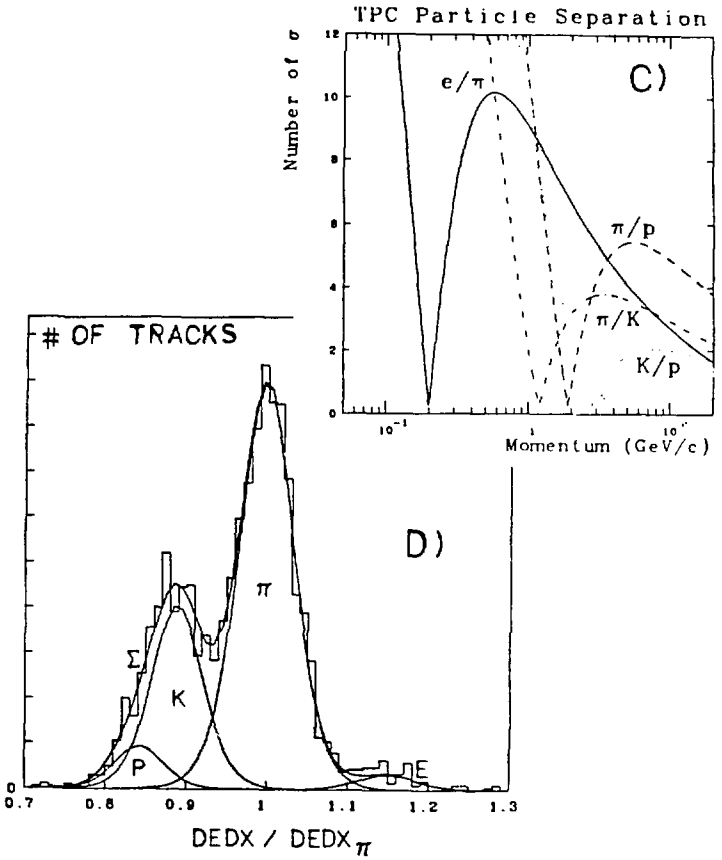

2. c) Calculated separation between particle types (in standard deviations), as a function of momentum, for tracks with at least 80 dE/dx samples. d) Ratio of measured dE/dx to the expected dE/dx for pions, for momenta between 3.5 and 6 GeV/c. The lines represent the contributions from protons, kaons, pions and electrons.

The fact that the TPC is the first storage ring detector using dE/dx for particle identification over the full momentum range warrants a more detailed description of the system.

The ionization electrons from tracks passing through the TPC drift axially under the influence of an electric field to endcap sectors, where they are detected in multiwire proportional chambers (fig. 3). Each of the up to 183 dE/dx samples is obtained from the pulse height of the corresponding wire, corrected for the track length seen by the wire, the wire gain, the electronic gain and the electron capture along the drift distance. The calibration of the gain is obtained in situ in three positions along each wire using remotly controlled Fe55 sources. A gain map taken before the detector was assembled allows interpolation between these three points. The pulse heights are also corrected for variations in the gain due to changes in gas density and purity and are continously monitored using minimum ionizing pions.

The ionization energy loss has a broad spectrum with a long high energy (Landau) tail; many samples, therefore, are needed to define an effective dE/dx. In practice we define dE/dx for each track to be the mean of the smallest 65% of the individual samples. To ensure an accurate particle identification, each track was required to have at least 80 dE/dx samples.

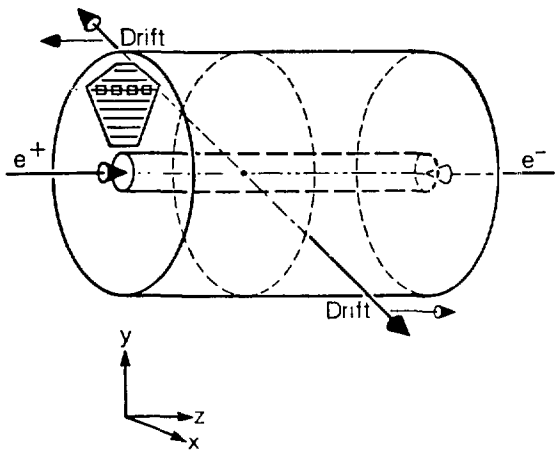

XBL 8310-754

3. Schematic view of the TPC. Track ionization formed in the sensitive volume drifts to arrays of proportional wires (only one set of wires shown). Position in the bending plane (x,y) is found from signals induced on cathode pads beneath the wires.

Fig. 2b) shows the distribution of dE/dx vs momentum for events where e+e- annihilate into hadrons. In the low-momentum region below 1 GeV/c, the pion, kaon and proton bands are well separated. Above 1 GeV/c the dE/dx resolution of 3.7% (for tracks with at least 80 dE/dx samples) is comparable to the differences in dE/dx for the various particle types, and the bands overlap. At 3.5 GeV/c, for example, the separation in dE/dx is 3.5 standard deviations for pions and protons, and 1.4 standard deviations for kaons and protons (fig. 2c,d). Most of the particles in the horizontal electron band in fig. 2b) result from photon conversions in the 0.2 radiation lengths of material before the TPC.

4) Data sample and event selection

The experimental data discussed in this paper correspond to an integrated luminosity of approximately 29 pb^{-1} at a center of mass energy of 29 GeV.

For the selection of annihilation events and the subsequent anaylysis, "good" charged tracks were defined requiring that the extrapolated orbit passes the nominal interaction point within +- 10 cm in the beam direction and within 6 cm in the plane perpendicular to the beam; only tracks at polar angles between 30 degr. and 150 degr. and with a well- measured momentum were accepted.

An event candidate had to have at least 5 good charged tracks, not including electrons from photon conversions which were eliminated based on their dE/dx in the TPC or by geometrical reconstruction. In order to remove two photon and beam gas events, the total energy E_{ch} of the charged particles (including electrons) had to exceed one half the beam momentum, and the sum of the momentum components along the beam direction had to be less than 40% of E_{ch}. 3-prong tau decays were removed by requiring at least one jet in the event having either more that 3 non-electron tracks, or an invariant mass above 2 GeV.

Two examples of typical multihadron events, as observed in the TPC detector, are shown in fig. 4).

From the number of hadronic events corrected for effects of initial state radiation, and the integrated luminosity determined from Bhabha events in the calorimeters, we obtain a value for R, the ratio of the measured total hadronic cross section to the muon pair cross section, of 3.7 +/- 0.4. This value is in good agreement with the results of measurements made by other detectors at similar energies at PEP and PETRA [5].

5) Inclusive Hadron Production

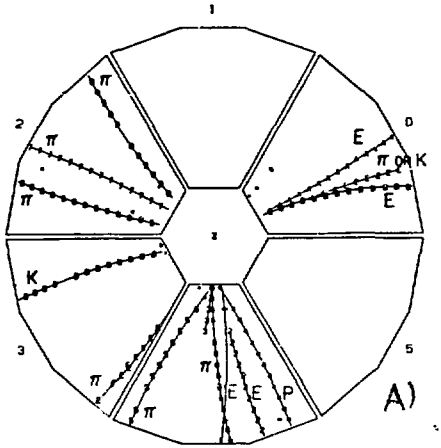

4. Typical hadronic events in the TPC detector: a) view along the beam line, shown are the pad-hits and the corresponding track fits. As indicated in the figure, except for one all particles are unambigiously identified by their ionization energy loss.

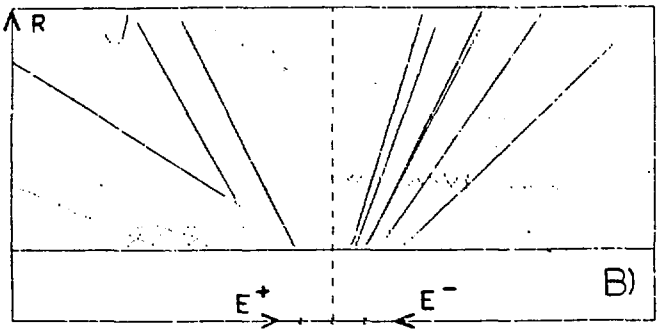

b) View of wire-data in the r-z plane. All 6 wegdes of the TPC folded on top of each other.

As a first step the understanding of the fragmentation process of quarks and gluons into hadrons requires the knowledge of the production cross sections of pions, kaons and protons in e+e- annihilation at high energy.

Fig. 5) shows the inclusive cross sections for charged hadron production. In the low-momentum region the raw numbers of pions, kaons and protons were obtained by counting tracks in the bands corresponding to the various particle types in fig. 2b); at high momentum a maximum likelihood fit to the dE/dx distribution was used (fig. 2d). As an input to this fit, the position of the average dE/dx as a function of velocity was determined from independent measurements of cosmic muons and conversion electrons to better than 0.3 %. The cross sections shown in fig. 5) are corrected for detector acceptance and for the effects of the event selection and of initial state radiation; the errors shown are dominated by systematic uncertainities.

In order to simplify the comparison with other experiments, and to eliminate uncertainties related to the (at present) rather limited accuracy of the luminosity measurements, we present the results on inclusive cross sections normalized to the total annihilation cross section into hadrons, i.e. in terms of fragmentation functions.

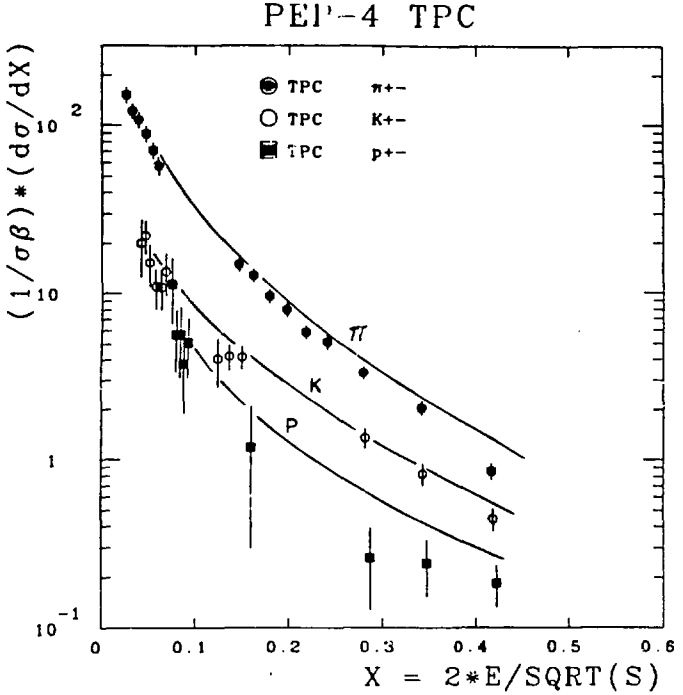

TPC: 29 GEV PRELIMINARY DATA

5. Normalized differential cross section $(1/\sigma\beta)/(d\sigma/dx)$ for charged pion, kaon and proton production in e+e- annihilation at 29 GeV cms energy. X is defined as the hadron energy scaled by the beam energy. The solid lines represent predictions from the LUND fragmentation model for s/u = 0.3.

Included in fig. 5) are predictions from the LUND-model for quark and gluon fragmentation [6]. The model calculations use the standard parameters, including a production ratio of s and u quarks in color strings of 0.3. The agreement with our measurements is quite good; using the kaon inclusive cross section, s/u can be constrained to 0.3 +- 0.1.

Fig. 6) shows the fraction of pions, kaons and protons among charged hadrons, in comparison with earlier data from TASSO [7]. Our measurements comfirm the rise of the kaon and proton fractions with increasing momentum, although even at the highest momentum baryon production is still strongly suppressed relative to pions and kaons. Note that most of this rise is explained by phase space effects and as a result of resonance decays, which tend to soften the pion spectra more than the spectra of heavy hadrons [8]. The observed spectra are e.g. consistent with a constant baryon/meson ratio for the primarily produced hadrons , if a vector/scalar ratio of 1 is assumed.

The particle ratios and fragmentation functions given in figs. 5,6) include decay products of particles with lifetimes below $5 * 10^{-10}$ sec.

The photon detection in the hexagonal calorimeter allows the reconstruction of neutral pions. The π^0 spectrum can then be compared with the charged pion spectrum. Fig. 7a)

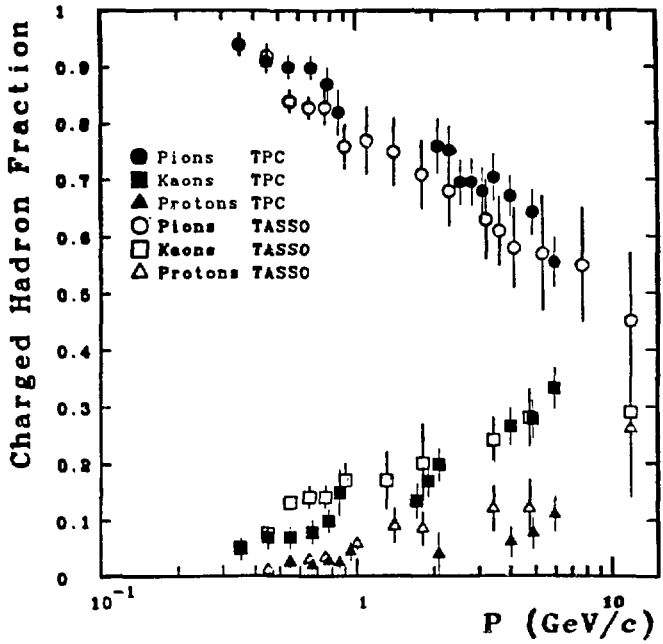

TPC: 29 GeV Preliminary Data TASSO: 34 GeV

6. Charged hadron fractions vs momentum for pions, kaons and protons, for the TPC and TASSO[7] experiments. For the TPC data, the error bars shown are dominated by systematic effects.

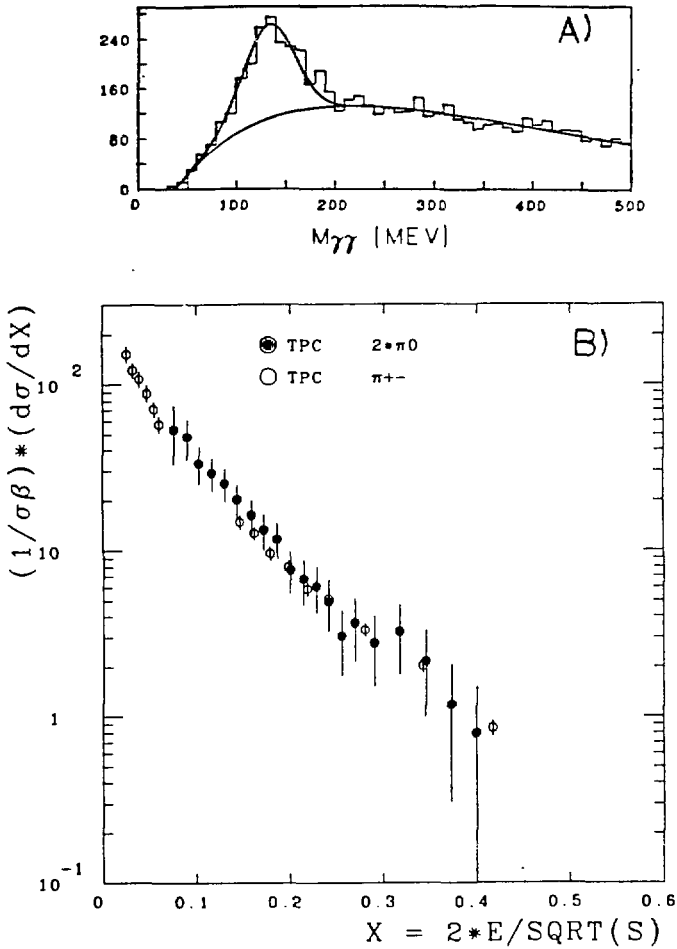

7. a) Distribution for the 2-photon invariant mass from the hexagonal calorimeter. b) Normalized cross section for inclusive piO-production at 29 GeV cms energy, compared to the inclusive cross section for charged pions.

shows the distribution of 2-photon invariant masses, for photon energies above 500 MeV. A clear peak is seen at the π^0 mass, with a width of 26 MeV rms. The background under the π^0 peak was estimated from Monte-Carlo simulations, and from events with a fake photon generated by flipping one photon into the opposite jet and combining it with real photons.

The resulting π^0 cross sections agree well with previous measurements [9]. It is compared with the inclusive charged pion cross section in fig. 7b). Within the errors, the two agree as expected from isospin symmetry.

6) Particle Fractions in 3-Jet Events

The fragmentation functions and particle ratios presented in the previous chapter are averages over all types of jets generated in e+e- annihilation, i.e. all quark flavors and gluon jets. The next question is to which extent the properties of quark jets depend on the flavor of the parent quark - we shall return to that question in chapter 9 -, and especially if gluon jets differ from quark jets.

We have extracted a sample of 3-jet events using a clustering method [10]. The lowest momentum jet ('jet 3') in these events has a probability of 55 % of being a gluon jet, as compared to 30 % for the medium-momentum jet ('jet 2'). For these events, the pion fractions were determined

for fast particles (p) 2 GeV/c). These fast particles can be unambigiously assigned to a jet and should be sensitive to the type of parton generating the jet. Because of the limited statistics, kaons and protons could not be separated for that sample.

The resulting pion fractions, 73+-4 %, 68+-4% and 69+-7% for jets 1, 2 and 3, respectively, are consistent with being the same for all three jets. However, the numerical values cannot be compared directly, since the fractions are measured at different scaled momenta (z) in the jets. In fig. 8) the pion fractions are displayed as a function of the mean z of the particles contributing to the data point, along with the inclusive pion fraction in hadronic events. For the 3-jet events, z is the momentum of a particle scaled to the jet momentum (which is derived from the angles between the reconstructed jet axes); for the inclusive ratios, the particle momenta are scaled to the beam momentum. Assuming that the particle fractions in quark jets approximately scale in z, the pion fraction in the lowest-momentum ('gluon') jet is slightly higher than in the high momentum jets. A drastic enhancement of heavy hadron production in gluon jets can be excluded (note that we are only sensitive to the sum of kaon + proton production; an increase in the baryon rate, as seen in Upsilon decays [11], is still possible provided the kaon rate is reduced correspondingly).

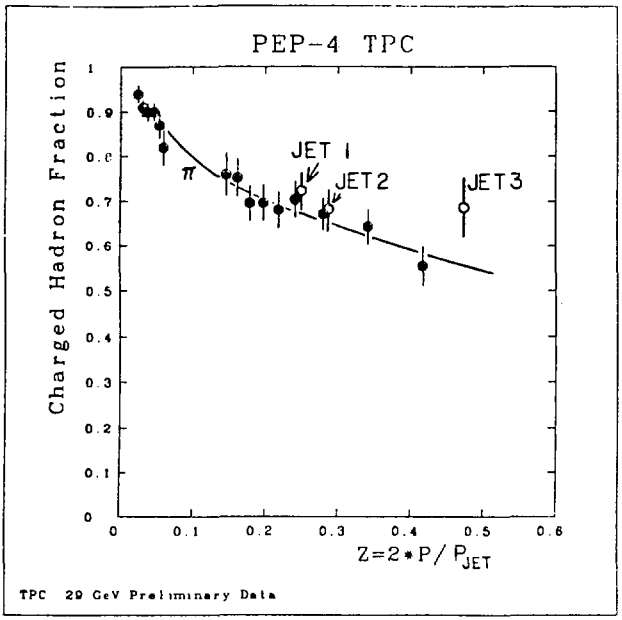

8. Fraction of pions among particles with p $\rangle$ 2 GeV/c in jets 1, 2 and 3 in 3-jet events. The fractions are plotted at the average z of hadrons with p $\rangle$ 2 GeV/c in the corresponding jet. For comparison, the inclusive pion fraction as a function of z (= particle momentum / beam momentum) is included.

At first, this result may seem surprising, since the (flavor-blind) gluon is expected to generate more leading strange mesons than for instance a u-quark. A more detailed study however shows, that this 'advantage' is offset by strange particle production in the s, c, and b jets produced in e+e- annihilation. Standard fragmentation models like the LUND model reproduce our result.

7) Search for fractional charged objects

Results from quark searches in matter have cast some doubts on the dogma of perfect quark confinement; on the other hand fractional charge searches at accelerators (largely concentrated on production of charge 1/3 and 2/3 particles) have set rather stringent limits. Recently, however, models have been proposed [12] in which color triplets are confined, yet some states with higher order representations of SU(3)color are unconfined; one could e.g. have free charge 4/3 diquarks.

Using the dE/dx information, the TPC detector is well suited to look for stable particles with unusual signatures, e.g. fractionally charged particles.

A first search in hadron events of 22 pb^{-1} integrated luminosity yielded 50 candidate tracks with high momentum and unusally high energy loss. The main background source for that sample consists of unresolved pairs of nearby tracks,

which fake a single track with twice the expected ionization.

The fine spatial segmentation of the TPC allowed us to develop a series of cuts to reduce this background, based on the widths of the pad and wire hits [13]. These cuts reject all candidates, while retaining good efficiency for protons with similar dE/dx.

Fig. 9) shows the limits on inclusive production of stable charge 4/3 particles in hadronic events [13], along with results of a similar search by JADE [14]. The limits depend on the assumptions for the inclusive production spectra and on the mass of the object; they are typically of the order $5 * 10^{-3}$ for flat momentum distributions.

Preliminary limits of similar order have been obtained for inclusive production of charge 2/3 objects.

8) Inclusive Resonance Production in e+e- Annihilation

The investigation of resonance production in e+e- annihilation yields additional information on quark fragmentation beyond what can be learned from the study of stable hadrons:

1. Since most of the stable particles are decay products, the spectra of direct hadrons are more relevant for an understanding of the fragmentation process.

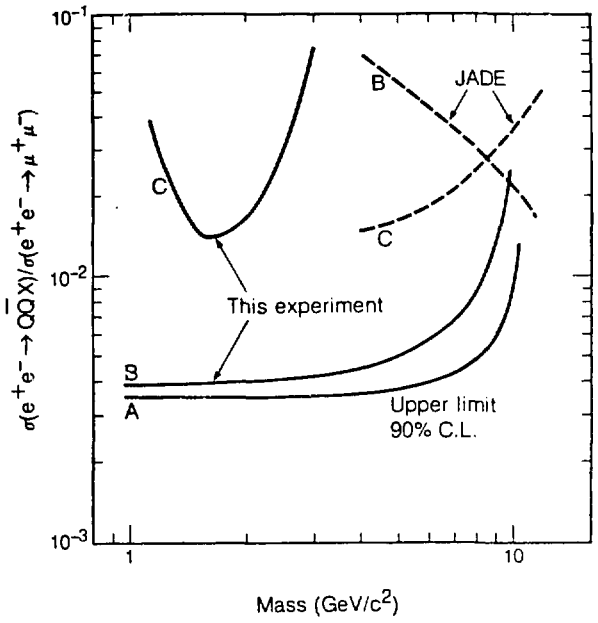

XBL 8310 752

9. Limits on the inclusive production cross section for charge 4/3 objects, scaled to the muon-pair cross section, as a function of the mass of the object. The curves represent different momentum distributions: a) dN/dp = p**2/E, b) dN/dp = constant, c) dN/dp = (p**2/E)*exp(-3.5*E). The dotted lines show limits from a similar search performed by JADE [14].

2. Phenomenological models [15] 'predict' the mass spectrum of hadrons produced in e+e- annihilation.

3. The fraction of vector mesons, as well as other parameters are inputs in most of the 'standard' fragmentation models like [6].

We will report here on inclusive k*0 and 0 production.

To search for resonances, dE/dx-identified hadrons were used. In momentum regions where hadrons cannot be identified unambigiously , the probability for a particle to be of a particular kind was calculated from the difference of its measured dE/dx and the known average dE/dx for that kind at the given momentum. These probabilities were weighted with the measured particle fractions (fig. 6). A minimum (weighted) probability for the best assignment was required for particles used in the mass combinations. No further cuts were applied except for a standard track selection.

Figs. 10a) and 10b) show the invariant mass distributions for unlike-sign k-pi and k-k combinations, respectivly, together with fits of a resonance shape and a background taken from like-sign combinations. Clear K^{*0} and ϕ signals are visible.

The inclusive k^{*0} and ϕ cross sections (normalized to the total cross section) are shown in fig. 11) along with the spectra of kaons; also included is a prediction by the

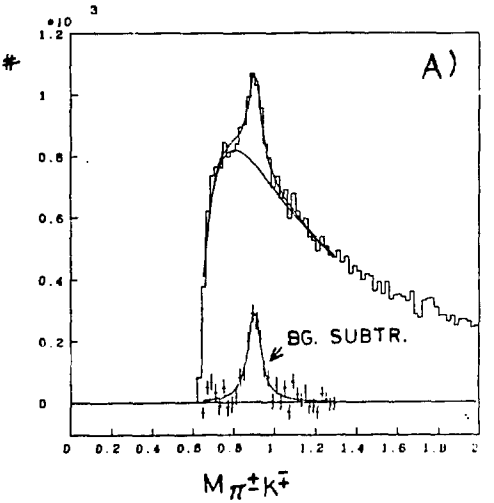

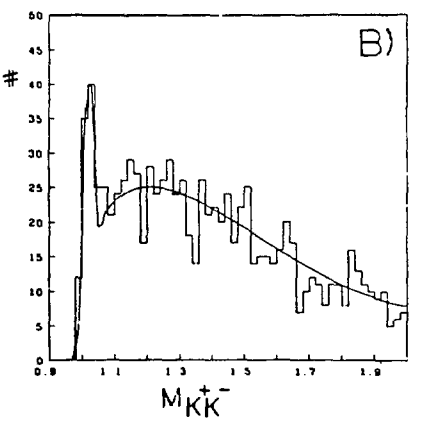

10. a) Mass spectrum of unlike-sign k-pi combinations. b) Mass spectrum of k+k- combinations. The full lines are fits using a Breit-Wigner resonance shape and a background shape derived from like-sign combinations. The particles are identified by dE/dx.

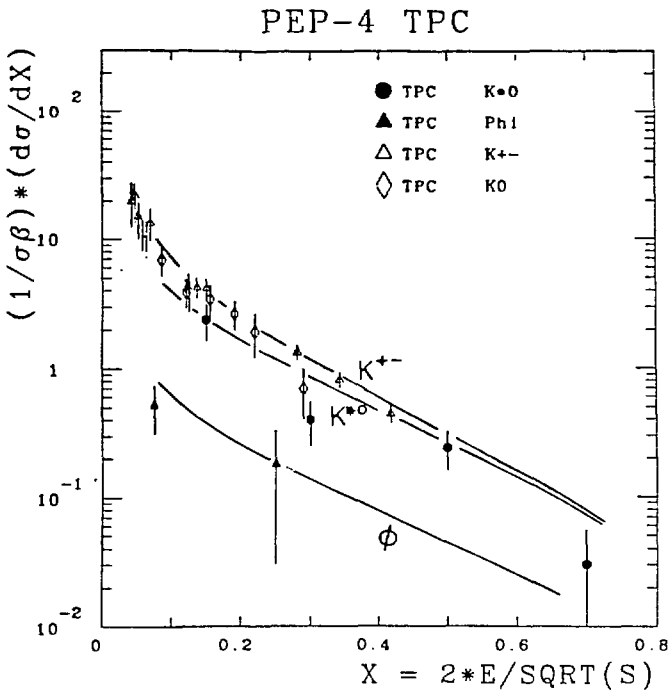

TPC: 29 GEV PRELIMINARY DATA

11. Inclusive cross section for k*0 and ϕ production in e+e- annihilation at 29 GeV, normalized to the total hadronic cross section. Also shown is the spectrum of kaons, and predictions from the LUND model using s/u = 0.3 and v/s = 1.

LUND model [6] using a vector/scalar ratio of 1 and $s/u = 0.3$.

At high momentum, k^{*0} and normal kaons are produced at similar rates, in agreement with the model calculation. Production ratios of 3:1, as expected from the spin weights, are clearly excluded. It is furthermore interesting to note that the model gives a reasonable description of ϕ production, indicating that the mechanism of OZI suppression, which is built in implicitly, is appropriate.

9) Long-Range Correlations in e+e- annihilation

From the previous discussion it seems obvious that in order to gain deeper insight into the mechanisms of parton fragmentation, the study of inclusive particle production has to be supplemented by other techniques.

The recent observation of strong long-range correlations (LRC) in proton-antiproton interactions, and the increase of the strength of the correlations with the cms-energy [16], which proves that LRCs are not a non-asymptotic phenomenon, has revived the interest in LRCs in electron-positron annihilation.

The term "long-range correlations" refers to the observation that the properties of the two jets in an event - the "beam" and the "target" jet in p-p and in pbar-p interactions, and the "quark" and the "anti quark" jet in

e+e- annihilations - are correlated, and that these correlations have a large range in rapidity, in contrast to the well- known short-range correlations (SRC), whose strength decreases exponentially with increasing separation in rapidity.

In the following, we shall adopt the usual (historical) notation and refer to the two jets as to the "forward" (F) and "backward" (B) jets, "forward-backward" (FB) correlation will be used as a synonym for LRC. The forward jet is defined as the ensemble of particles having rapidities $y \geq 0$ in the overall cms, with y referring to the sphericity axis of the event. Correspondingly, particles with $y < 0$ form the backward jet.

In general, FB-correlations can have different origins:

1. The reaction investigated represents an average over many different processes. This is the case in hadron-hadron interactions, where particles are produced in inelastic collisions with different impact parameters. Similarly, the production of different quark flavors in high energy e+e- annihilation should result in LRCs if there are differences in the jets produced by different quark species.

2. True dynamical long range correlations. If color confinement bears some analogy to a phase transition, one expects LRCs, which could be interpreted as coherent fluctuations of the "string tension" in a color flux tube [17]. On the other hand, such LRCs are inconsistent with one of the postulates of the quark-parton-model (QPM), namely that the fragmentation of a parton is independent of its production - except for SRC-effects, of course.

3. Correlations of purely kinematical origin due to phase-space restrictions. These correlations should be negligible provided that the cms energy is very large compared to the masses and transverse momenta of the hadrons involved.

Experimentally, a FB correlation coefficient C can be defined as follows (we use the FB multiplicity correlation as an example):

$$C = (NF*NB) - (NF)*(NB)$$

NF and NB denote the hadron multiplicities in the forward and backward jets, respectively. The standard way to present FB correlations is to study the dependence of (NF) on NB. Any FB correlation is characterized by a non-zero slope S:

$$S = d(NF)/dNB$$

S and C are related via

$$S = C/(SF*SB)$$

where SF and SB represent the rms width of the NF and NB distributions.

Assuming that in e+e- annihilation the production of different quark flavors is the only potential source for LRCs, it is easy to show that C is always 0 or positive; and that C**1/2 is a measure for the rms variation of the mean hadron multiplicity over the different jet flavors [18].

A measurement of C or S therefore provides a new tool in the investigation of parton fragmentation [18]: a result C (0 would indicate that basic assumptions of the parton model are violated; on the other hand, C)= 0, supplemented with the assumption of independent fragmentation, measures differences in the fragmentation properties of the various quark flavors. Of course, as we shall see, the study of LRCs is not restricted to multiplicity correlations. Identical arguments hold for LRCs between the mean transverse momentum of particles in jets, the inclusive fragmentation functions, etc [18].

The main experimental problem in the study of LRCs is given by the fact that any non-ideal detector tends to induce artificial correlations between jets, e.g. due to the

requirement of a minimum number of particles seen in the detector in order to accept an event. This is demonstrated in fig. 12), where (NB) is shown as a function of NB for normal hadronic events. The negative correlation at low multiplicities is purely artificial; in addition, part of the (small) positive correlation at high multiplicities is due the correlated detector acceptances for two back to back jets.

In the present analysis, great care has been taken to avoid such biases. For example, each event was devided in two jets, each of which had to pass separate acceptance cuts; only events with two 'good' jets were used. Each jet was required to be contained well within the fiducial area of the detector, and to have a minimum momentum, number of particles etc. Events clearly inconsistent with a 2-jet structure were rejected; the contamination in the event sample due to tau-tau and 2-photon events is below 1.1 %. Such a selection should avoid any problems of the type evident from fig. 12); various checks have been performed using both data and Monte-Carlo models to ensure that this is actually the case.

To reduce the influence of short range effects on the FB-correlation, a rapidity gap of one unit was introduced between the forward and the backward regions; only particles with $|y| \geq 0.5$ were taken into into account.

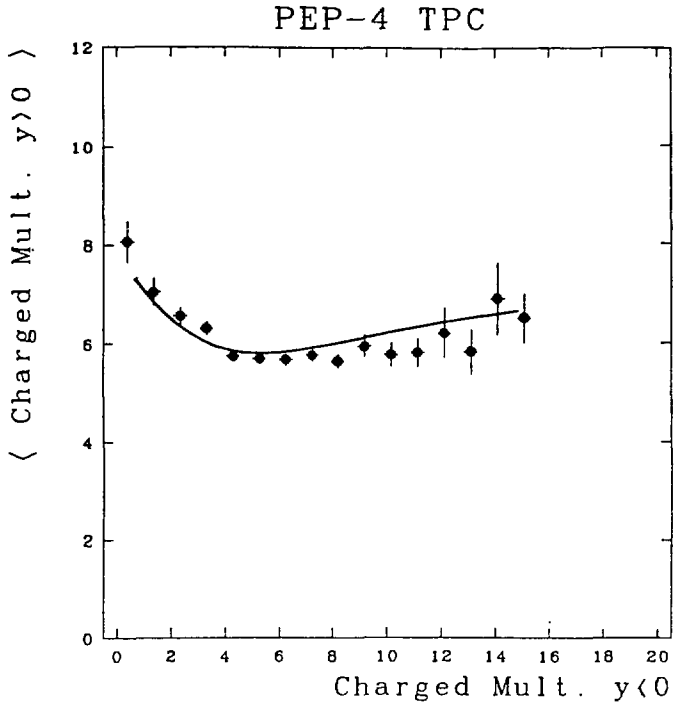

PRELIMINARY

12. Mean multiplicity in the "backward" jet as a function of the multiplicity in the "forward" jet, for hadronic events with at least 6 charged tracks.

Fig. 13) shows the FB correlation S for some typical properties of jets, like the multiplicity of charged hadrons, the jet mass, the mean scaled momentum of hadrons in a jet, their mean rapidity, mean pseudorapidity and mean transverse momentum. As expected in the basic quark-parton-model, all correlations were either consistent with 0 or positive . Assuming that true dynamical LRCs are absent [19], these values of S demonstrate the universality of transverse momentum scales in jets, and the non-universality of longitudinal fragmentation functions for different quark species.

Summary

Based on particle identification by ionization energy loss new measurements of inclusive pion, kaon and proton production in e+e- annihilation at 29 GeV are reported. The inclusive production of particles with unusual ionization, like charge-2/3 or charge-4/3, is excluded at a level of less than 10^{-2} .

For the first time at PEP and PETRA energies, inclusive production of k^{*0} and ϕ has been studied. All inclusive spectra and particle ratios agree reasonably well with predictions from the LUND model using s/u = 0.3 and v/s = 1.

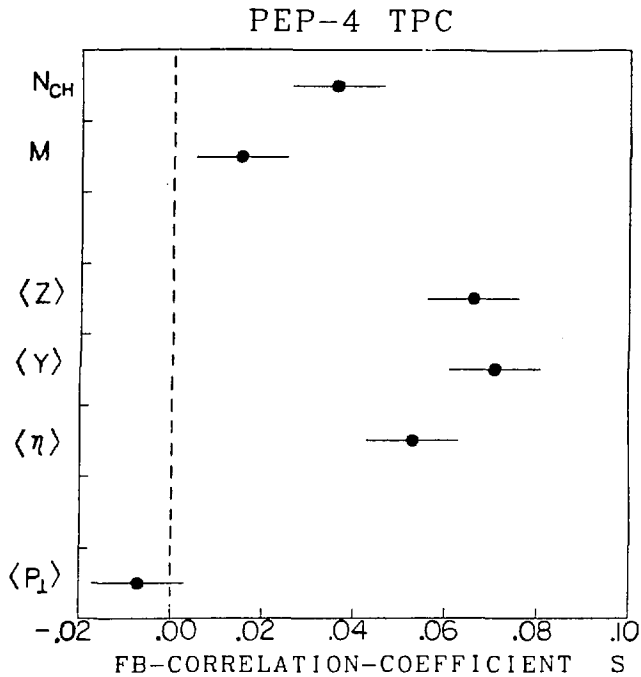

PRELIMINARY

13. Forward-backward correlation coefficient S (see text) for the hadron multiplicity Nch in jets, jet masses M, mean scaled momentum ⟨z⟩, mean rapidity ⟨y⟩, mean pseudorapidity ⟨η⟩ and mean transverse momentum ⟨$p_\perp$⟩. The systematic error due to remaining detector effects is estimated to +- 0.01 (not included in the error bars).

Long range correlations of particles in jets have been exploited to investigate differences in the fragmentation of the various quark species.

Due to the limited space, many interesting topics like the entire area of 2-photon physics had to be omitted in this presentation. Nevertheless it is obvious that the special capabilities of the TPC open new and interesting possibilities even in a field as crowded as the physics of e+e- annihilation at PEP and PETRA energies.

Acknowledgements

This work was supported in part by the United States Department of Energy under contracts DE-AC03-76SF00098, DE-AM03-76SF00034, by the National Science Foundation, and by the Joint Japan - United States Collaboration in High Energy Physics.

References

1. (see title page)

2. Proposal for a PEP facility based on the time projection chamber; John Hopkins University, Lawrence Berkeley Lab., University of California at Los Angeles, University of California at Riverside, Yale University (1976)

3. CELLO Collab., H.J. Behrend et al., DESY 82-061 (1982) and H.J. Behrend, Proc. of the 21st Int. Conf. on High Energy Physics, Paris (1982)

4. TPC Collab., H. Aihara et al., IEEE Trans.Nucl.Sci. NS-30 (1983) 63; NS-30 (1983) 67; NS-30 (1983) 76; NS-30 (1983) 117; NS-30 (1983) 153

5. JADE Collab., W. Bartel et al., Phys.Lett. 129 (1983) 145
TASSO Collab., R. Brandelik et al., Phys.Lett. 113B (1982) 499
MARK J Collab., B. Adeva et al., Phys.Rev.Lett. 50 (1983) 499
MAC Collab., M. Picollo, Talk at the SLAC Summer Institute on Particle Physics, Stanford, CA (1983)

6. B. Andersson, G. Gustavson, C. Peterson, Z. Phys. C1 (1978) 105
B. Andersson, G. Gustavson, Z. Phys. C3 (1980) 223
B. Andersson, G. Gustavson, T. Sjoestrand, Z. Phys. C6 (1980) 235
T. Sjoestrand, Computer Phys. Com. 27 (1982) 243

7. TASSO Collab., M. Althoff et al., Z.Phys. C17 (1983) 5

8. B. Andersson, G. Gustavson, C. Peterson, Nucl.Phys. B135 (1978) 273

9. CELLO Collab., H.J. Behrend et al., Z.Phys. C14 (1982) 189
TASSO Collab., R. Brandelik et al., Phys.Lett. B108 (1982) 71

10. A. Baecker, Z.Phys. C12 (1982) 161

11. DASP-II Collab., H. Albrecht et al., Phys.Lett. 102B (1981) 291
CLEO Collab., P. Avery et al., Paper submitted to 1983 Int. Symp. on Lepton and Photon Interactions, Cornell

12. R. Slansky, T. Goldman, G. Shaw, Phys.Rev.Lett. 47 (1981) 887
A. DeRujula, R. Giles, R. Jaffe, Phys.Rev. D17 (1978) 285

13. TPC Collab., H. Aihara et al., submitted to Phys.Rev.Lett.

14. JADE Collab., W. Bartel et al., Z.Phys. C6 (1980) 295

15. R.D. Field, S. Wolfram, Nucl.Phys. B213 (1983) 65
T.D. Gottschalk, Nucl.Phys. B124 (1983) 201;
CALT-68-1052 (1983);
M.G. Bowler, Z.Phys. C11 (1981) 169

16. UA5 Collab., K. Alpgard et al., CERN-EP/83-20 (1983)

17. J.H. Kuehn, H. Schneider, Z.Phys. C8 (1981) 115

18. P. Hoyer, SLAC-PUB-3166 (1983)

19. Note that in the LUND model partons fragment independently in the sense used in this article; the string fragmentation scheme doesn't introduce significant LRCs (relative to the LRCs due to the differences in heavy and light quark fragmentation).